Paper 43

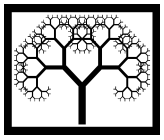

Proceedings of the Eleventh International Conference on Computational Structures Technology,
B.H.V. Topping, (Editor),
Civil-Comp Press, Stirlingshire, Scotland

Collapse of Carbon and E-Glass Composite Tubes under External Hydrostatic Pressure

P.T. Smith, A.P.F. Little and C.T.F. Ross
School of Engineering
University of Portsmouth, United Kingdom

Abstract

This paper describes a number of investigations, both experimental and theoretical, into the collapse of 32 composite tubes, each of circular cross-section, under the application of external hydrostatic pressure; for the first time. These investigations were on the collapse of fibre reinforced plastic tube specimens, sixteen of which had been manufactured from fifteen carbon layers, and sixteen of which were manufactured from nine E-Glass layers. This work is of much importance for deep diving submarines; especially for large diameter submarines, which are required to conquer the Mariana Trench. The theoretical work was carried out using separate finite element computer programs, as follows:

1. The 'in house' finite element computer program, called 'The Buckling of Composite Layer Analysis Method' (BCLAMB). This program used 2, 3 & 4 Gauss points, to test for numerical instability, due to 'locking'.
2. Another finite element computer program, called 'Poseidon'; which was created to overcome the limitations of BCLAMB; namely the fact that only twenty layers of fibres were permissible with BCLAMB, for each specimen.
3. Lastly, the commercially available finite computer program ANSYS, using Shell 93 and Shell 99. This program had the big advantage of providing quite spectacular graphical displays.

At this point in time, it is convenient to mention that the British Standard 5500 code (PD 5500), does not have the capability of being able to analyze multi-layered composite shells, buckling under external hydrostatic pressure, nor does the literature published by the principal United Kingdom (UK) classification society, namely Lloyds of London. Hence, the work presented in this paper is both novel, and of use to industries, concerned with external pressure vessel construction, using composite materials; especially the resulting design charts provided in this paper, for the first time. This work of buckling composite tubes was backed-up by the models, which were tested to destruction.

The experimental investigations carried out illustrated that the composite tube specimens tested, behaved in a manner comparable to isotropic and composite models previously tested, in that the vessels of short length, suffered collapse through axisymmetric deformation, whilst the intermediate length vessels collapsed through inelastic instability, and the long slim vessels collapsed through elastic instability. Moreover, it was determined that the models suffered failure at changes of the composite lay-up, as a consequence of the manufacturing process used for the models in question. The changes of the composite lay-up of the material had the appearance of being the weak points of the composite tube specimens.

Keywords: ANSYS, BCLAMB, finite elements, circular cylinder, buckling, axisymmetric yield, composites, external pressure, submarines.

1 Introduction

The surface area of the Earth is about 196.9 million sq.mi (510 million km^2), and about 75% of it is covered by water, but despite this, only about 0.1% of the oceans' bottoms have been explored by Dickens et al [1]. Such research has found large quantities of precious metals and minerals, together with large quantities of methane hydrates. In the case of methane, Dickens et al [1] have found deep-sea frozen methane hydrates lying under the ocean bottoms at depths of 2 miles (3.22km) or more. According to Dickens et al, the quantity of this methane is about 10,000 billion tones, and if it is divided amongst all of mankind, it will amount to about 1,670 tonnes per person on Earth, or in monetary terms about $1,500,000 per person on Earth. Thus, it is necessary to exploit the oceans' bottoms, which are as deep as 7.16 miles (11.52 km).

Currently, a large submarine can only dive to a depth of about 400m (1312 ft), but the deepest part of the oceans is 29 times deeper than this. As the submarine dives deeper and deeper into the oceans, the external hydrostatic pressure increases, so that the wall thickness has to be increased. Eventually, the wall thickness becomes so large that the vessel has no reserve buoyancy and will sink like a stone to the very bottom of the ocean. Ross[2] has found that for a submarine of internal diameter 10m (32.81ft) and constructed in high-tensile (HY80) steel, the thickness of its hull will be about 2.3 m (7.58ft), if it is to be designed to dive to the bottom of the Mariana's Trench. The only way to overcome this problem is to use a material with a higher strength: weight ratio than high-strength metals. Such materials are Glass Fibre Reinforced Plastic (GFRP) and Carbon Fibre Reinforced Plastic (CFRP). There are many other composites, which are suitable, but these are cheaper than many of the other composites and have been used successfully for other structures.

2 Background

2.1 Buckling

Under uniform external pressure a long thin-walled circular cylinder can fail by non-symmetric bifurcation buckling or shell instability, at a fraction of that to cause axisymmetric yield [1]. To increase the buckling resistance of such vessels, they are usually stiffened by ring stiffeners, spaced at suitable distances apart. If the ring stiffeners are not strong enough, the entire vessel can collapse bodily by a mode called general instability. Another mode of failure is called axisymmetric deformation, where the vessel keeps its circular form while imploding.
For long thin vessels, the shell instability failure mode usually occurs at a much smaller pressure than that required to cause axisymmetric yield. The extremely long thin circular cylindrical vessel will fail in a flattening or ovalling mode, but the shorter circular cylinder will buckle in a lobar mode. In this paper, we will concern ourselves only with shell instability and axisymmetric deformation.

2.1.1 Thinness Ratio and Plastic Knockdown Factor

Windenburg and Trilling [3] introduced a thinness ratio (λ) to consider the fall in theoretical elastic buckling pressures due to the fact that shorter vessels failed by inelastic instability. The effects of initial out-of roundness of these cylinders can cause a further drop in their buckling pressures than that predicted by elastic theory for perfect vessels. This factor is needed because even slight deviations from the perfect geometry can reduce the buckling pressure of a pressure vessel considerably. With the thinness ratio, it is also required to determine the so-called plastic knockdown factor (PKD) [2] from the experimental results, so that the Design Chart can be made.

2.2 Finite Element Method (FEM)

In the theoretical analyses of these vessels, we will consider shell instability using an in-house finite element computer program called BCLAM, together with the well-known computer package ANSYS. For both programs, the possibility of using different material models, including orthotropic material properties is allowed for.

2.3 The Composite Tubes

The models used for the tests were manufactured from fibre reinforced plastic tubes; see (Figures 1 & 2).
The models consisted of sixteen carbon and sixteen e-glass models. The manufacturer was Carbon Fibre Tubes Ltd, Hayling Island, UK. The lay-up was 0°/90°/0°/90°/0, for both the carbon and e-glass models, with the layers being laid lengthwise (0°) and circumferentially (90°).
The manufacturer describes the manufacturing process to be rather similar to that of making a Swiss roll.

Figure 1: The PTSC carbon models and their end bungs

Figure 2: The PTSG e-glass models

That is the layers were of cloth form and were wrapped around each other, with impregnated resin, in a circumferential manner.
For sealing the two ends of each specimen under external water pressure, two end bungs with 'O' rings had to be manufactured. These end bungs were manufactured out of mild steel and are shown in Figure 1. The actual number of layers was 15 for the carbon models and 12 for the E-Glass models, with the layer thicknesses were calculated from the overall measured wall thickness of 3.2 mm, where:

E1 = Young's modulus of the layer in direction of the fibre
E2 = Young's modulus of the layer perpendicular to the fibre direction
G12 = in-plane shear modulus

2.3.1 Material Properties of the Single Layers

The experimentally obtained properties of the single layers are shown in Table 1:

	E_x (MPa)	E_y (MPa)	G_{12} (MPa)	σ_{yp} (MPa)	ν_{12}	No. of Layers	Layer Thickness (mm)
Carbon	25593	13348	5546	3300	0.28	16	3.0
E-glass	33920	33920	4546	1100	0.28	12	3.0

Table 1: Experimentally Obtained Material Properties of the Composite (MPa)

Where: E_x = Young's Modulus in the x-direction; E_y = Young's Modulus in the y-direction; σ_{yp} = Yield Stress in the direction of the fibre; υ_{12} = Major Poisson's ratio.

2.4 Experimental Analysis and the Design Charts

After calculating a series of theoretical buckling pressures and thinness ratios, with the aid of an in-house computer program, namely MisesNP [2], for the both the PTSC Series and PTSG Series models made from carbon and e-glass respectively, the respective buckling pressures of the 32 models in total were determined experimentally. MisesNP adopts the von Mises analytical solution for simply-supported ends.
This testing was done in a high-pressure tank, where each model was tested to failure and the experimental buckling pressure was noted. With the experimentally obtained values for the buckling pressure (P_{exp}) of the series it was possible to calculate the PKD using (Eq. 1):

$$PKD = P_{cr}/P_{exp} \tag{1}$$

With the values of PKD and the previously calculated thinness ratios (λ) it was possible to generate a Design Chart, where $1/\lambda$ was plotted against PKD. This Design Chart could now be used to calculate the predicted (experimental) buckling pressure P_{pred} for a pressure vessel out of the same material for untested vessels. During the design process the factors PKD and λ have to be calculated. Once the design chart has been produced, it is possible to obtain the PKD from this chart, which then can be used to calculate the predicted buckling pressure, namely $P_{pred,,}$ using (Eq. 2):

$$P_{pred} = P_{cr}/PKD \tag{2}$$

The value of P_{pred} obtained using (Eq. 2) supplies a new value giving an approximation of the real buckling pressure, which can now be used to predict the possible diving depth of the submersible.

3 Experimental Investigation

3.1 Equipment

The experiments were carried out in the laboratories of the University of Portsmouth, using a high pressure testing tank (of 210 bar maximum pressure), with a pressure pump and pressure gauge (of 410 bar maximum pressure). Before the manufactured specimens were tested, they were checked for any defects due to the manufacturing process or any matters that could affect their performance during the testing. It was observed that all the test specimens had minor defects at the ends, when they were cut during manufacture. These defects had the appearance of small delaminations and cracks on the surface. The affected zones could be roughly sized between 0.5cm and 1cm lengths from the ends, for all specimens. Due to the supporting influence of the end bungs; these had shoulders of about 1cm penetrating into the specimens' ends, it was decided that these defects had almost no influence on the results. Some of the specimens, especially the shorter ones, had bigger defects. These could spread almost over the whole length of the specimens. The defects could have had a considerable influence on the strength of the models, particularly those with the larger defects and because of this; it was decided to carefully observe the behavior of the specimens with the larger defects during the tests.

3.1.1 Model Failure.

All models were observed before and after failure and pictures were taken for documentation. The most important information has already been given, but in addition to this, three other issues were found, namely that three major failure modes could be indicated during the testing. These failure modes could be related to the length of the models, with the first two failure modes being elastic buckling and inelastic buckling; see (Figure 3).

Figure 3: Inelastic buckling of a model.

The third failure mode being axisymmetric yield failure; see (Figure 4).

Figure 4: Axisymmetric deformation of a short model.

The longest models failed due to elastic buckling. In this failure mode the test models buckled elastically, but with a subsequent reduction of pressure the model returned to its original shape without any visible signs of damage. The medium sized models failed due to inelastic buckling. This meant that the deformation just prior to buckling was large, so that the material had 'yielded' and buckled inelastically. These models did not return to their original shapes after the pressure was decreased to zero. The shortest models failed due to axisymmetric 'yield' failure. In this case, the models deformed on the whole circumference; no lobes were formed in this mode, and the vessels collapsed axisymmetrically. This failure mode can be seen in Figure 3. It was found that the defects that were seen during the pre-test observation had almost no influence on the collapse pressures of the models. All the cracks, fractures or delaminations that could be seen on the models after collapse, were found at different locations to the deformations that were found just after manufacture and micro graphed; see (Figure 5).

Figure 5: A 'micrograph picture' of the Carbon/Glass material.

After a careful investigation of the failure modes of the models, some of the vessels were subjected to microscopic analysis, via a microscope (Figure 5), where the layer composition was photographed with magnified pictures of the polished surface perpendicular to the rotational axis of each tube. From these pictures, it could be seen that the lay-up of the different layers varied considerably over the whole circumference. After a check of the position of these lay-up modifications and the position of post-test fractures, it showed that both were in correlation. This could be seen on all specimens that fractured along the longitudinal axis.

4 Theoretical Investigations

As already stated in the previous section, the theoretical investigation was first done using BCLAM, an in-house DOS-based computer program and a derivative of BCLAM, namely Poseidon, created by the author, so as to overcome limitations of BCLAM. In this case, a truncated conical shell element was used with two ring nodes at its ends. Each ring node had four degrees of freedom, three translational and one rotational. The assumed displacement form in the azimuthal direction was sinusoidal and this enabled explicit integration in the azimuthal direction, thereby considerably reducing computational time.
In contrast to this, the ANSYS solution (ANSYS, 2005), used the Shell99 finite element, which had 8 nodes, with 6 degrees of freedom per node. Three of the degrees of freedom were translational and the other three were rotational degrees of freedom. The boundary conditions for both analyses were assumed to be simply-supported at the 'ends'.

5 Theoretical and Experimental Results

The results of the BCLAM, Poseidon and Shell99 analyses with the experimentally obtained material properties are listed in Table 2, where the figures in parentheses represent the number of circumferential waves or lobes (n) that the vessels buckle into. The thinness ratios had been calculated using the equivalent Young's modulus in y-direction and the other parameters listed in Table 2, with the wall thickness being set to for both the PTSC and PTSG Series of models. From Table 2, it can be seen that the ANSYS results are more stable than those yielded by BCLAM, especially for the very long and the very short vessels.

Using the results shown in Table 2, the design charts for the PTSC Series and PTSG Series of models are as shown in Figures 6 & 7.
As part of the results analysis, numerical instability was noticed, particularly in the case of the longer vessels, with 10 conical shell elements initially used for the BCLAM and Poseidon analysis and when this was increased to 12 conical shell elements, the calculated buckling pressure appeared to converge.

However, when the number of elements was increased to 20, the value of the calculated buckling pressure appeared to wildly diverge; similar experiences were observed for the very short vessels. Thus, it was believed that both BCLAM and Poseidon are unstable, probably due to a numerically unstable feature commonly called 'locking', Zienkiewicz [4]. With the experimentally obtained buckling pressures (P_{exp}) and the theoretically calculated buckling pressures (P_{cr}) of the previous sections, the plastic knockdown factors (PKD) for both approaches were calculated by (Eq. 1).

6 Conclusions

The experimental and theoretical investigations were performed successfully on the described fibre reinforced plastic tubes. The main findings from the investigations were:

Design Charts were created successfully for use with BCLAM, Poseidon and ANSYS Shell99, although, because of the numerical instability of the former, caution must be exercised. It should be emphasized here, that it appears that BS 5500 (PD 5500) does not exclusively cater for the buckling of thin-walled shells made from composite materials and this makes the present study a novel one.

Cylinder	Length L_0	$1/\lambda$	Pexp	BCLAM	Poseidon	ANSYS
PTSC1	240	0.218	8.625	14.1	14.2	13.0
PTSC2	230	0.223	8.525	14.3	14.4	13.2
PTSC3	220	0.228	10.204	14.5	14.5	13.5
PTSC4	210	0.233	10.351	14.8	14.8	13.8
PTSC5	200	0.239	10.531	15.1	15.0	14.2
PTSC6	190	0.245	10.750	15.4	15.4	14.6
PTSC7	180	0.253	11.000	15.8	15.9	15.2
PTSC8	170	0.259	12.500	16.4	16.4	15.9
PTSC9	160	0.267	13.140	17.0	17.0	16.8
PTSC10	150	0.276	13.125	17.8	17.8	17.4
PTSC11	140	0.285	13.254	18.9	18.8	17.4
PTSC12	130	0.296	13.564	20.3	20.3	17.6
PTSC13	120	0.308	13.657	22.2	22.2	17.7
PTSC14	110	0.322	13.500	23.6	24.1	17.8
PTSC15	100	0.338	13.500	25.0	26.0	17.8
PTSC16	90	0.218	8.625	26.4	27.9	17.8
PTSG1	240	0.080	2.59	3.577	3.577	3.848
PTSG2	230	0.081	2.41	3.747	3.756	3.971
PTSG3	220	0.083	2.41	2.748	3.899	4.117
PTSG4	210	0.085	2.43	3.749	4.083	4.294
PTSG5	200	0.087	2.47	4.492	4.491	4.509
PTSG6	190	0.089	2.50	4.855	4.854	4.771
PTSG7	180	0.092	2.94	5.299	5.299	5.096
PTSG8	170	0.095	3.51	5.849	5.673	5.501
PTSG9	160	0.098	4.42	5.735	5.765	6.014
PTSG10	150	0.101	4.44	6.046	6.047	6.109
PTSG11	140	0.100	4.53	6.453	6.454	6.843
PTSG12	130	0.108	4.68	6.728	6.929	7.275
PTSG13	120	0.113	4.72	6.995	7.545	7.305
PTSG14	110	0.118	4.89	7.262	8.161	7.335
PTSG15	100	0.123	4.89	7.529	8.777	7.365
PTSG16	90	0.080	2.59	7.796	9.393	7.395

Table 2. Experimental P_{exp} & the Theoretical Results (MPa & lengths, mm**).**

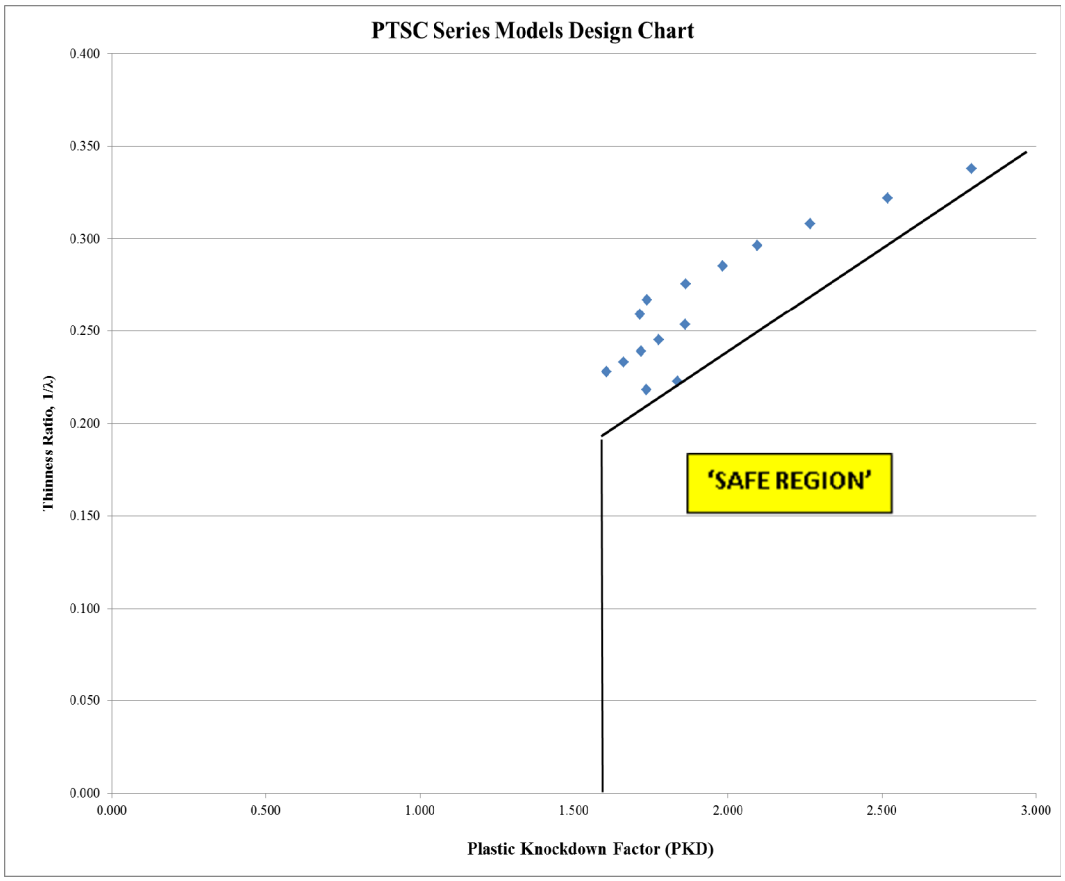

Figure 6: Design chart of the PTSC Series carbon models

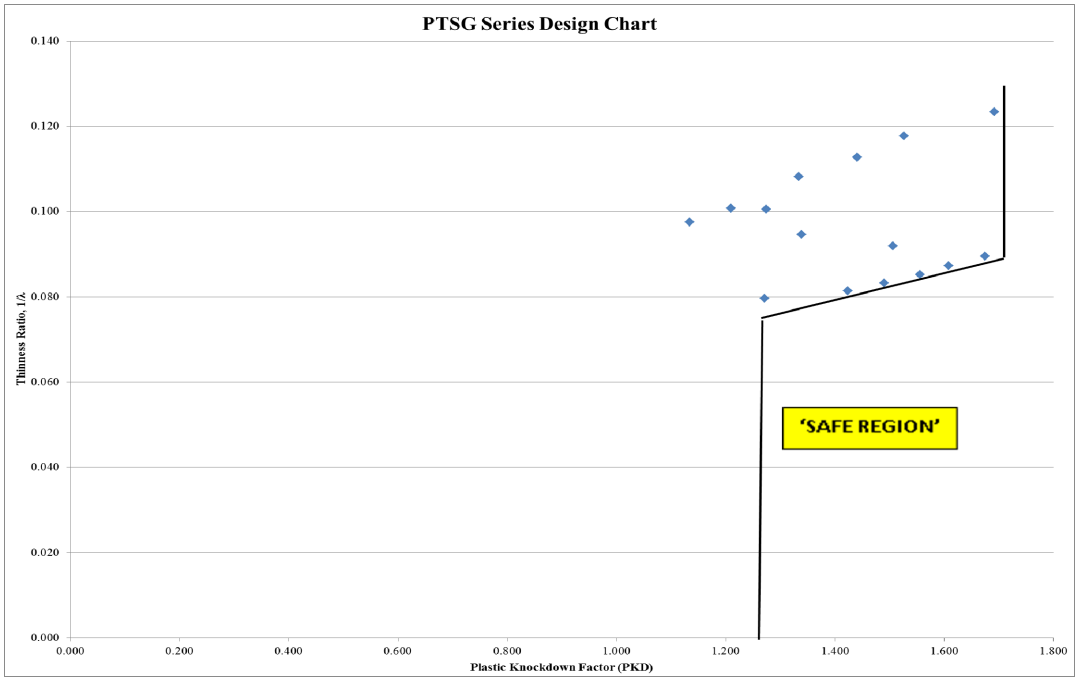

Figure 7: Design chart of the PTSG Series e-glass models

The tested models failed at locations where the lay-up of the single layers changed. These changes seem to reduce the strength of the composite in this location;
The Design Charts for the orthotropic composite materials have, in general a slightly different shape to design charts obtained for isotropic materials;

The Design Charts created in this paper should prove useful to designers, providing the structures have the same characteristics as those investigated herein, and a bigger safety factor is used.

References

[1] Dickens, Gerald, R., Paull, Charles, K., Wallace, Paul & The ODP LEG 164 SCIENTIFIC PARTY, Direct measurement of in-situ quantities in a large gas-hydrate reservoir, Nature, Vol. 385, 30th January 1997.

[2] Ross, C. T. F. Pressure Vessels: External Pressure Technology - 2nd Edition, Woodhead Publishers, Cambridge, U.K, 2011.

[3] Windenburg, D.F & Trilling, C, Collapse by Instability of Thin Cylindrical Shells under External Pressure. Trans., ASME, 11, pp 8 19-825, 1934.

[4] Zienkiewicz, O.C & Taylor, The Finite Element Method, Vols. 1 to 3, Butterworth-Heinemann, Oxford, U.K, 2000.

[5] ANSYS INCORPORATED, Release 10.0 Documentation for ANSYS. Canonsburg, USA, 2005.